Multi-modal Approach to Modeling Creep Deformation in Ni-Base Superalloys

Ridwan Sakidja[1], Wai-Yim Ching[2], Caizhi Zhou[3]

[1]Missouri State University
[2]University of Missouri at Kansas City (UMKC)
[3]University of South Carolina

Acknowledgement:
NETL(DOE) FE0031554

Federal Project Manager: Richard Dunst
Technology Manager: Briggs White

June 8th, 2021

Crosscutting Project Review Meeting High Performance Materials Program Review

Acknowledgment: This material is based upon work supported by the Department of Energy Award Number DE-FE0031554.

OUTLINES

1. Overview

2. Modeling Development based on the Electronic Structures:

- Bonding characteristics and elastic properties of carbide phases

3. Modeling Development at the Atomistic-Scale:

- EAM Potential Development utilizing High Entropy Alloy (HEA) Strategy
- Applications to γ (FCC) and γ + γ’ structure
- Phase stability analysis
- Applications to carbide structures

4. Modeling Development at the Continuum-Scale:

- Crystal plasticity model on void deformation
- Semi-empirical plasticity model on commercial superalloys

5. Summary and Path Forward

Multi-modal Approach to Modeling Creep Deformation In Ni-Base Superalloys

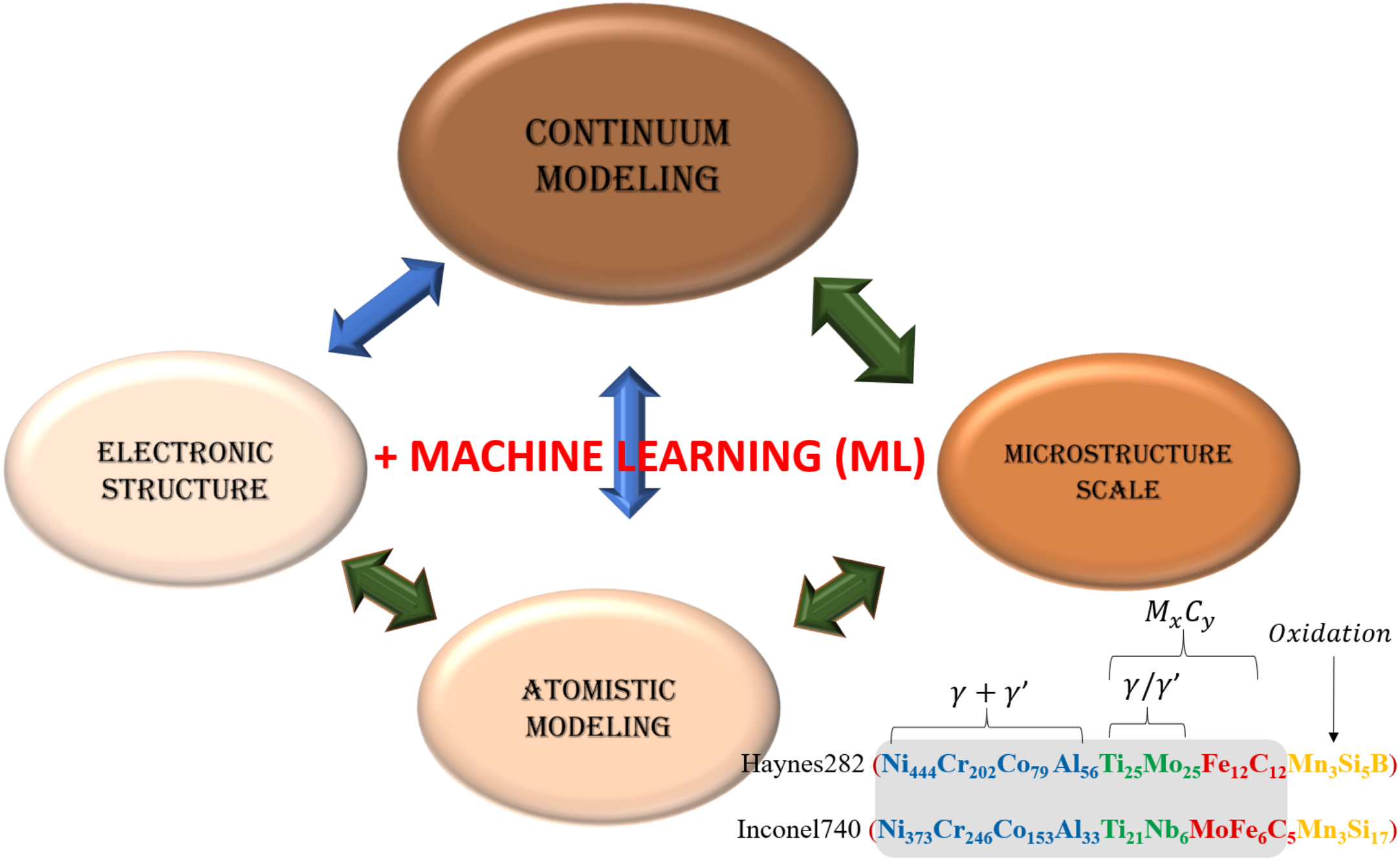

Electronic Structure-based Modeling:

- Predicting bonding characteristics & elastic properties

$M_{23}C_6$

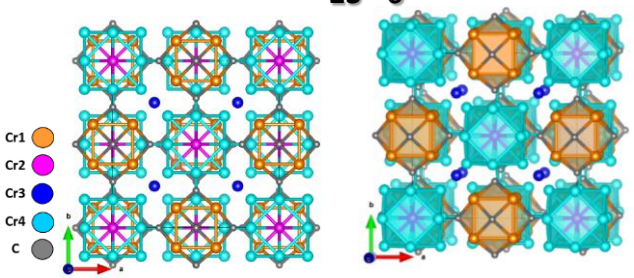

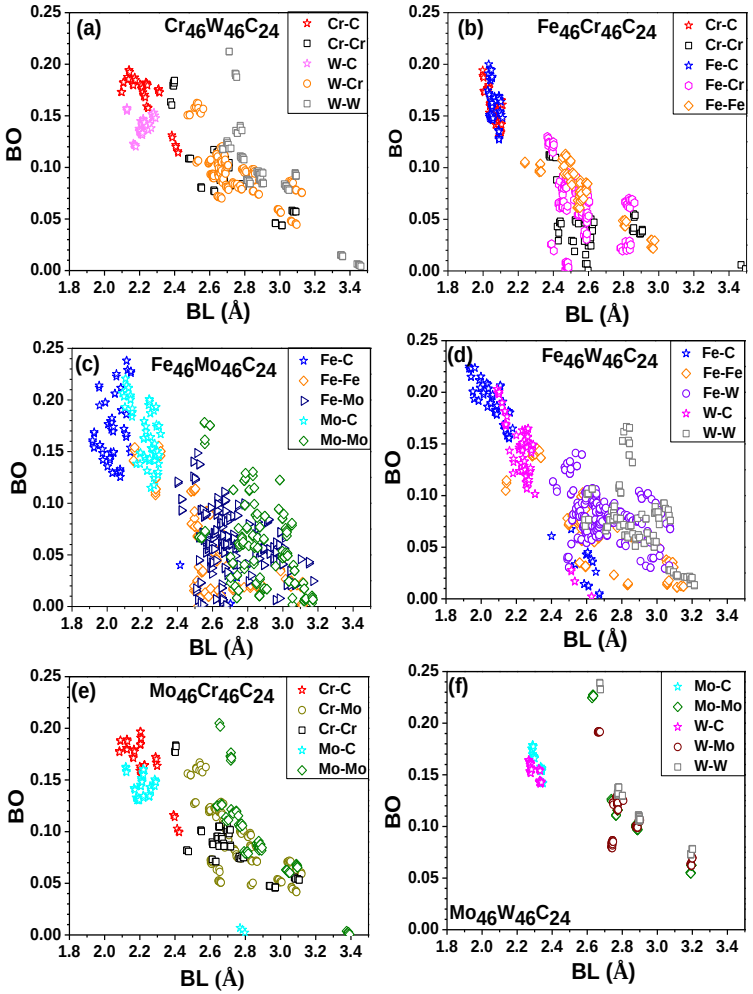

Bond order vs. bond length of ternary carbides

	C11	C12	C44	K	G	E	η	G/K	A^U	H
$Cr_{92}C_{24}$	472.15	211.53	124.88	298.427	126.63	332.82	0.3141	0.4243	0.0098	10.69
$Fe_{92}C_{24}$	432.09	246.42	58.24	308.414	69.65	194.32	0.3950	0.2258	0.3047	3.42
$Mo_{92}C_{24}$	457.24	220.09	113.51	299.138	116.28	308.81	0.3279	0.3887	0.0017	9.11
$W_{92}C_{24}$	510.38	252.59	136.12	338.521	133.14	353.12	0.3261	0.3933	0.0035	10.16
$Cr_{46}W_{46}C_{24}$	474.07	231.08	105.97	312.469	109.47	294.07	0.3431	0.3503	0.1488	7.76
$Fe_{46}Cr_{46}C_{24}$	471.16	221.87	118.87	304.802	122.98	325.19	0.3222	0.4035	0.0099	9.89
$Fe_{46}Mo_{46}C_{24}$	436.32	218.30	88.34	293.452	93.02	252.39	0.3567	0.3170	0.0786	6.17
$Fe_{46}W_{46}C_{24}$	466.93	241.65	92.20	314.966	96.88	263.60	0.3605	0.3076	0.1561	6.14
$Mo_{46}Cr_{46}C_{24}$	435.71	219.83	114.08	293.647	111.48	296.88	0.3315	0.3797	0.0591	8.61
$Mo_{46}W_{46}C_{24}$	482.57	232.39	111.06	317.581	115.47	308.95	0.3379	0.3636	0.0211	8.40

Calculated Cij, Shear modulus (G), bulk modulus (K), Young's modulus (E), Poisson's ratio (η), Pugh's modulus ratio (k = G/K), Universal anisotropy A^U and Vicker's Harness H

Electronic Structure-based Modeling:

- Developing models for multi-component γ and/or γ' structures

γ

Haynes 282

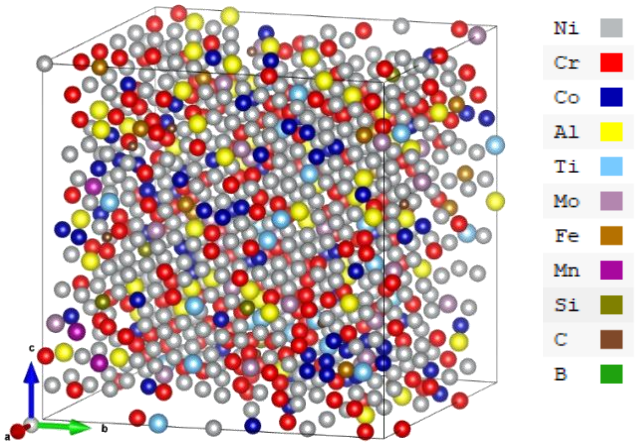

γ

Inconel 740

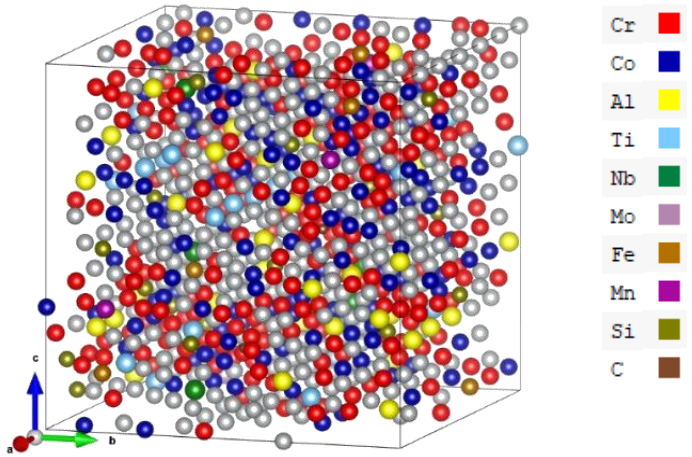

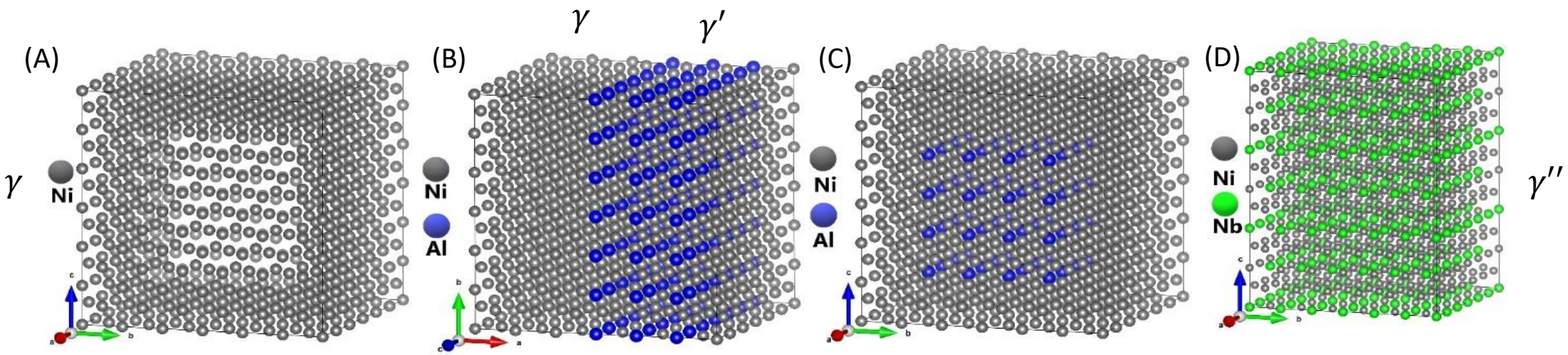

Superalloy models of (A) γ + vacancy (B) γ/γ' interface (C) $\gamma+\gamma'$, and (D) γ'' Ni_3Nb

Atomic-Scale Modeling:

➢Developing Interatomic Potentials for Superalloys using HEA strategy

MEAMfit
A reference-free modified embedded atom method (RF-MEAM)

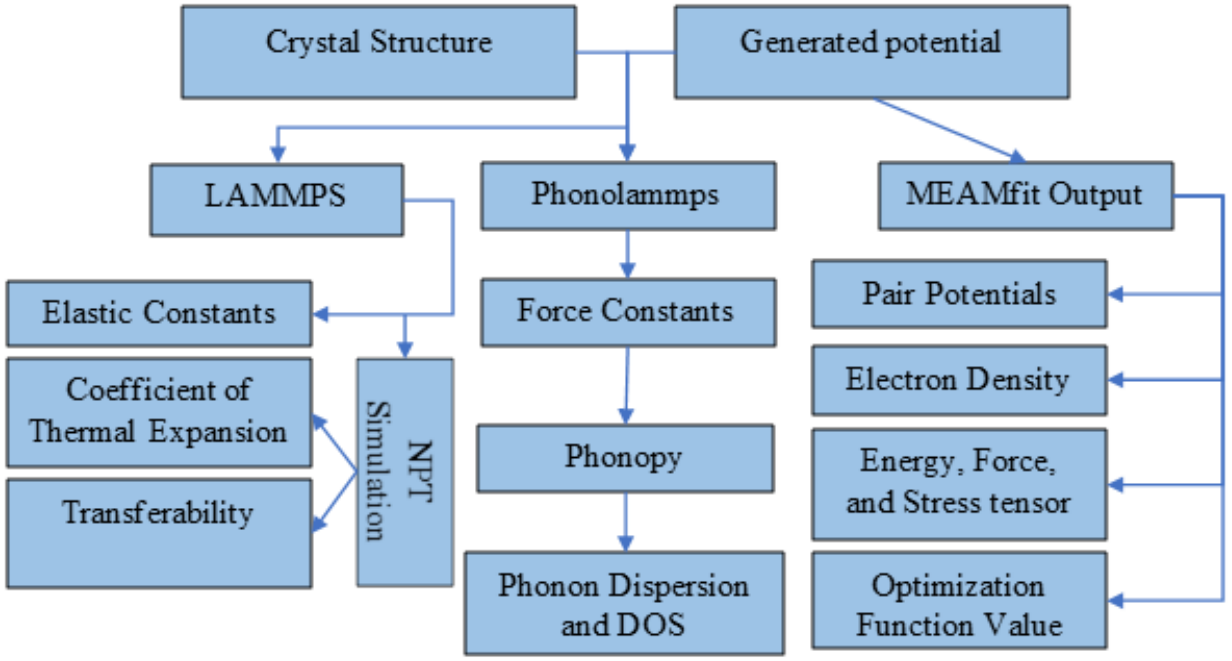

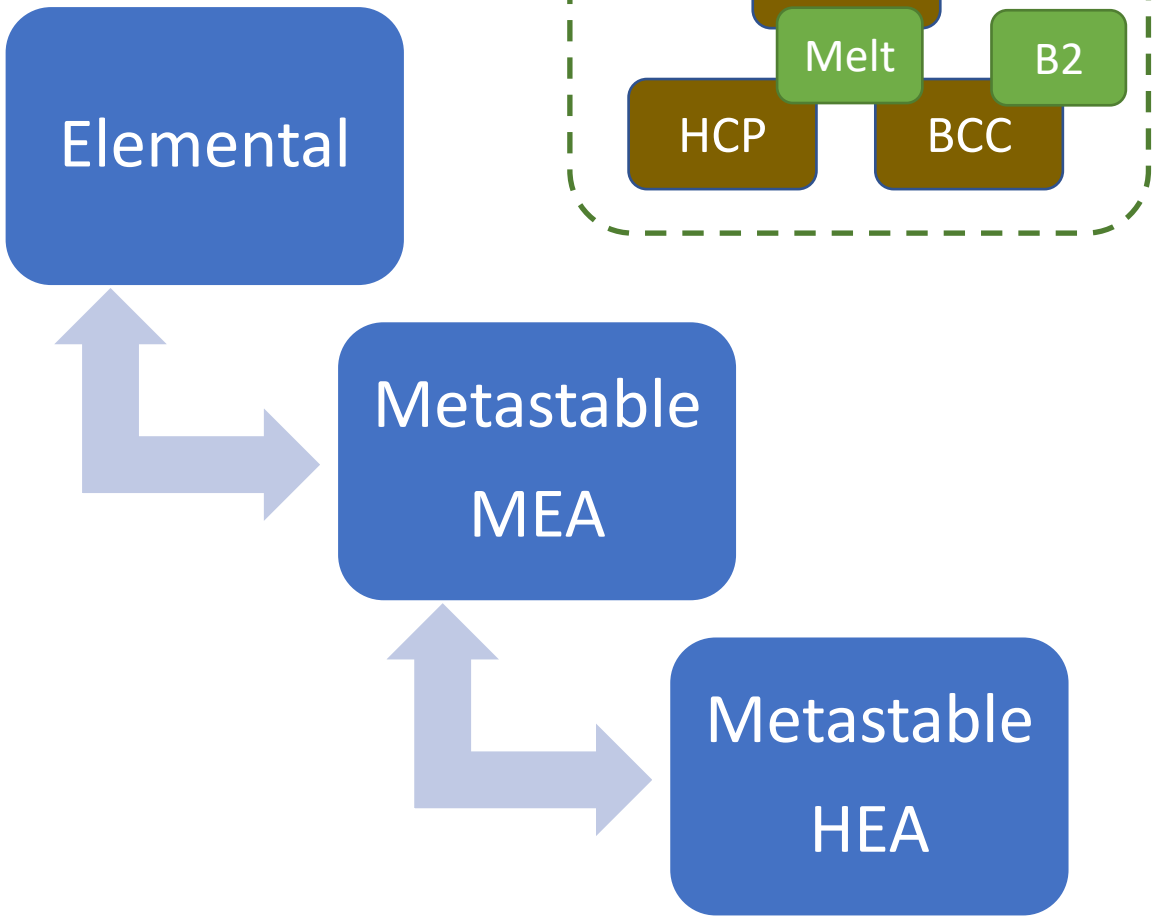

Andrew Ian Duff, M.W. Finnis, Philippe Maugis, Barend J. Thijsse, Marcel H.F. Sluiter, Computer Physics Communications, Vol. 196, pp. 439-445 (2015)

https://doi.org/10.1016/j.cpc.2015.05.016

Atomic-Scale Modeling:

➢Developing Interatomic Potentials for Superalloys using HEA strategy

General strategy: maximize combinations of energy, force & stress samplings derived from all types of atomic pairs

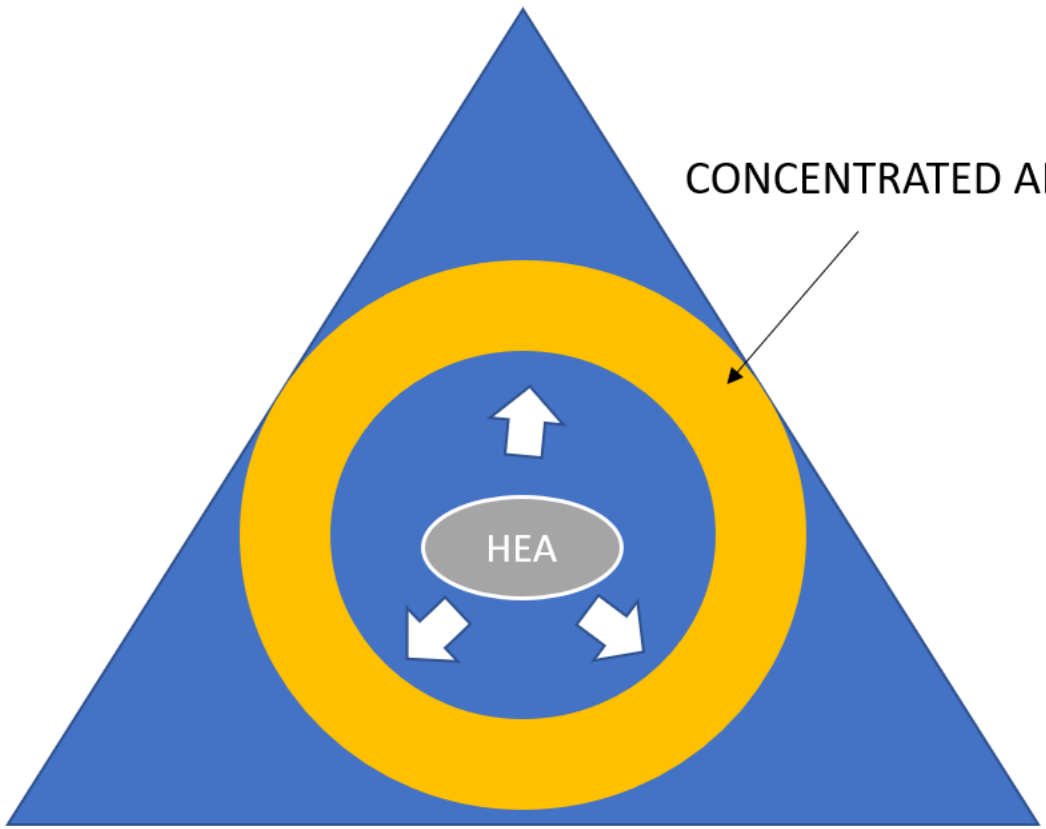

EXTENDED TO HIGHER-ORDER DIMENSIONS:

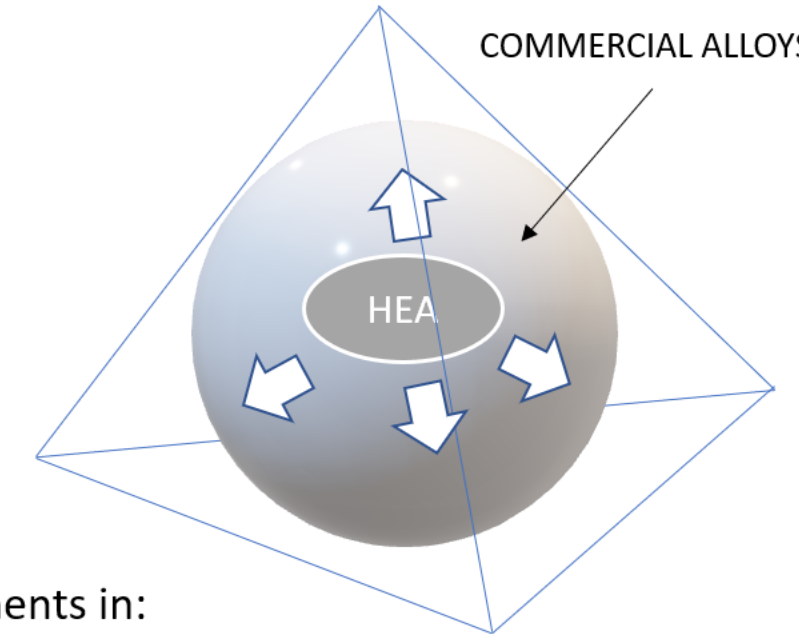

Major elements in:

Haynes 282: Ni-Cr-Co-Al-Ti-Fe-Cr-Mo-W-C

Inconel 740H: Ni-Cr-Co-Al-Ti-Fe-Nb-Mo-C

γ + γ' HEA: Ni-Cr-Co-Al-Fe-Ti-Nb

Hastelloy-N: Ni-Mo-Cr-Fe

High-T Steels: Fe-Cr-Ni-Mo-V-Nb-Mn-C

Atomic-Scale Modeling:

- Developing Interatomic Potentials for Superalloys using HEA strategy

Energy matching comparison:

FeNiCr

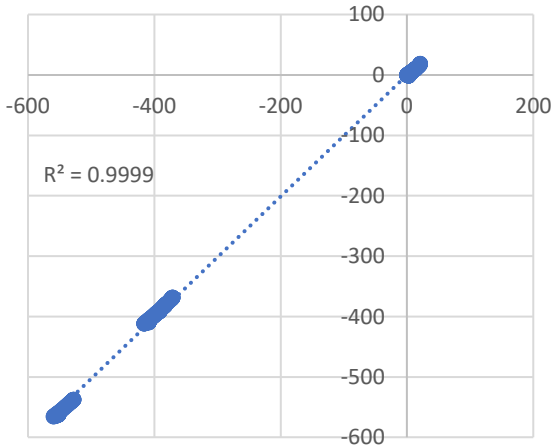

NiAlCo

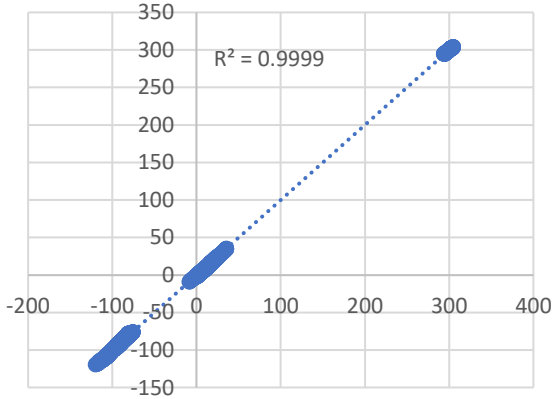

NiAlFe

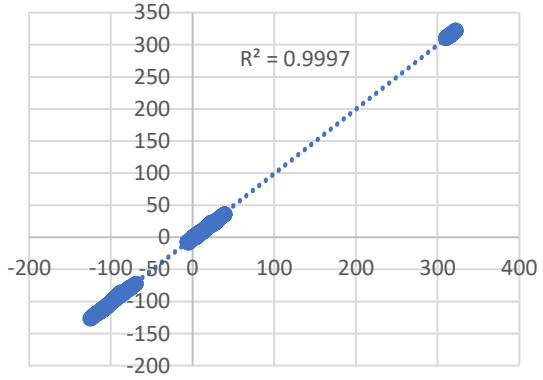

NiAlCuCoFeCr

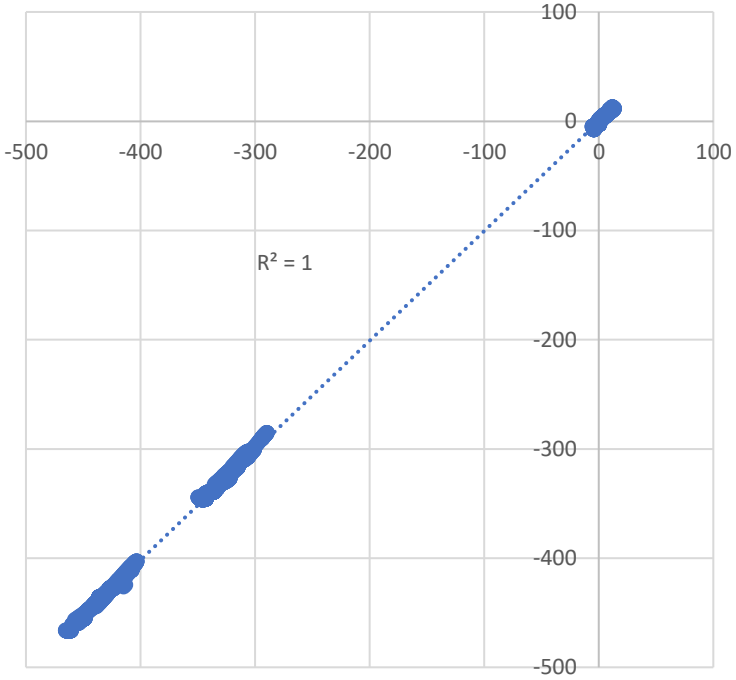

NiAlCr

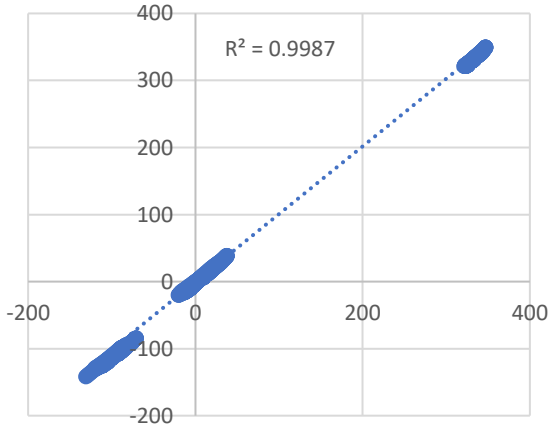

NiAlCu

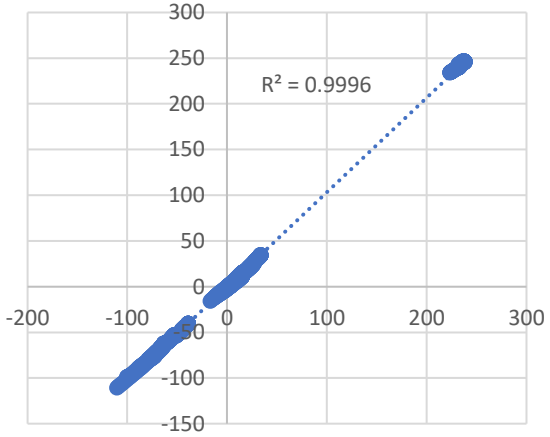

x axis : DFT and y axis: EAM

Atomic-Scale Modeling:

- Application to γ Structures

1000K

Thermal Stability Test on Polycrystalline Ni-Co-Cu-Fe-Ni-Cr Alloys

HEA-FCC

Al
Co
Cu
Fe
Ni
Cr

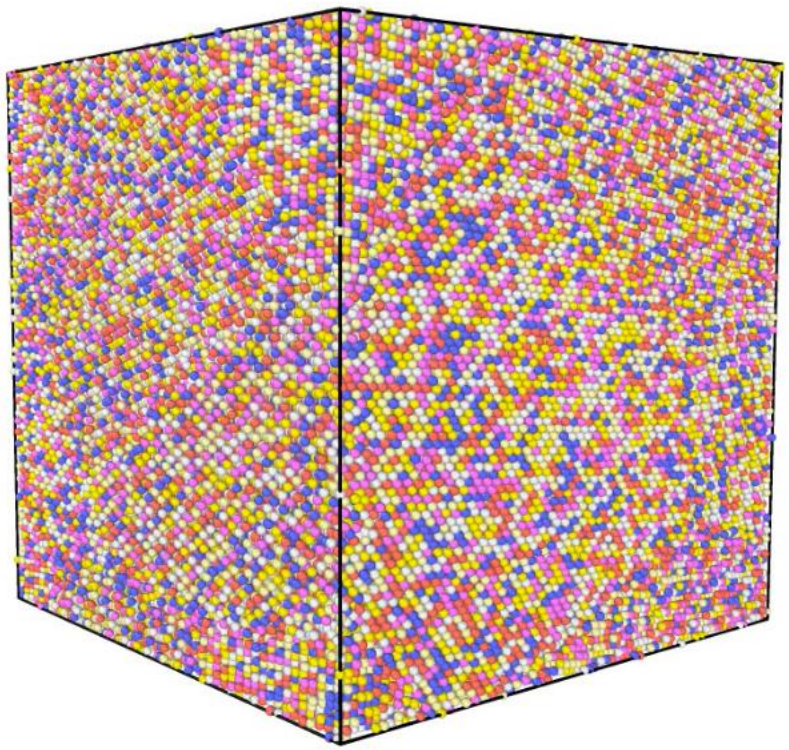

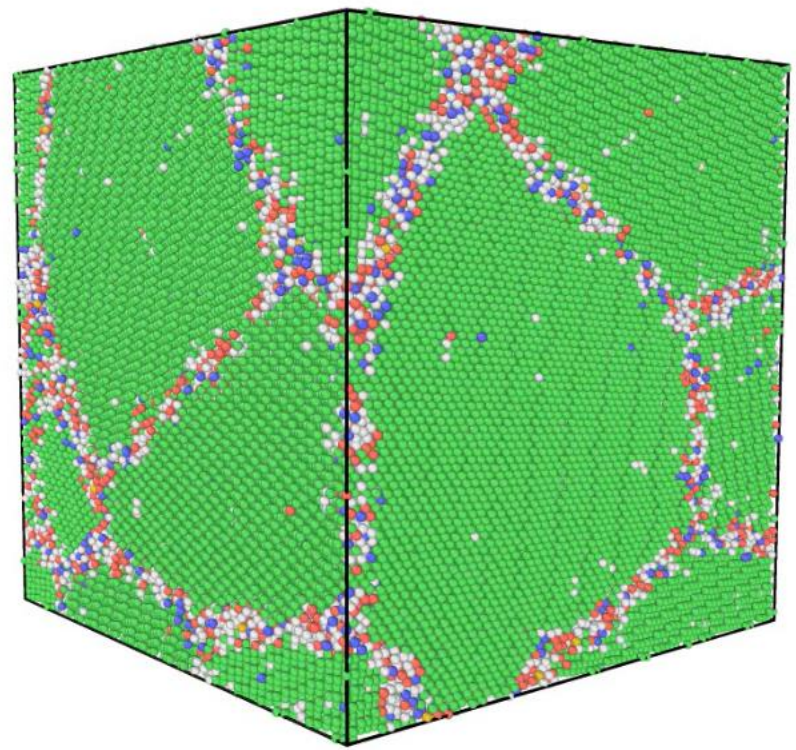

Atomic-Scale Modeling:

➢Developing Interatomic Potentials for Superalloys using HEA strategy

γ

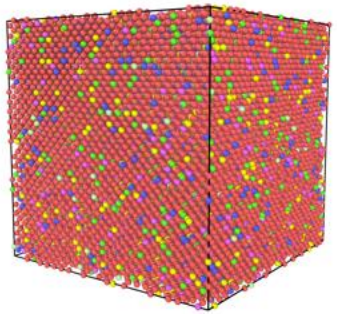

Haynes 282: Gamma Phase

300K

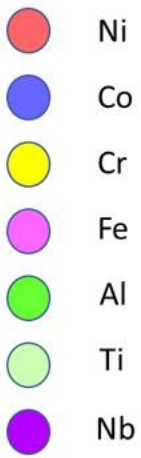

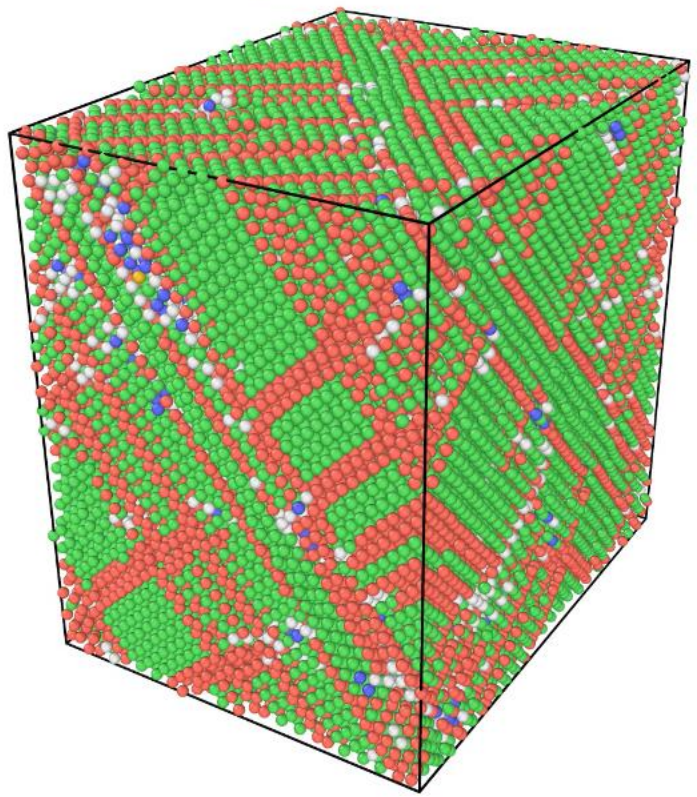

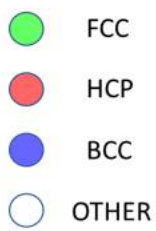

HEA-BASED EAM POTENTIAL: COMPOSITION & STABILITY TEST

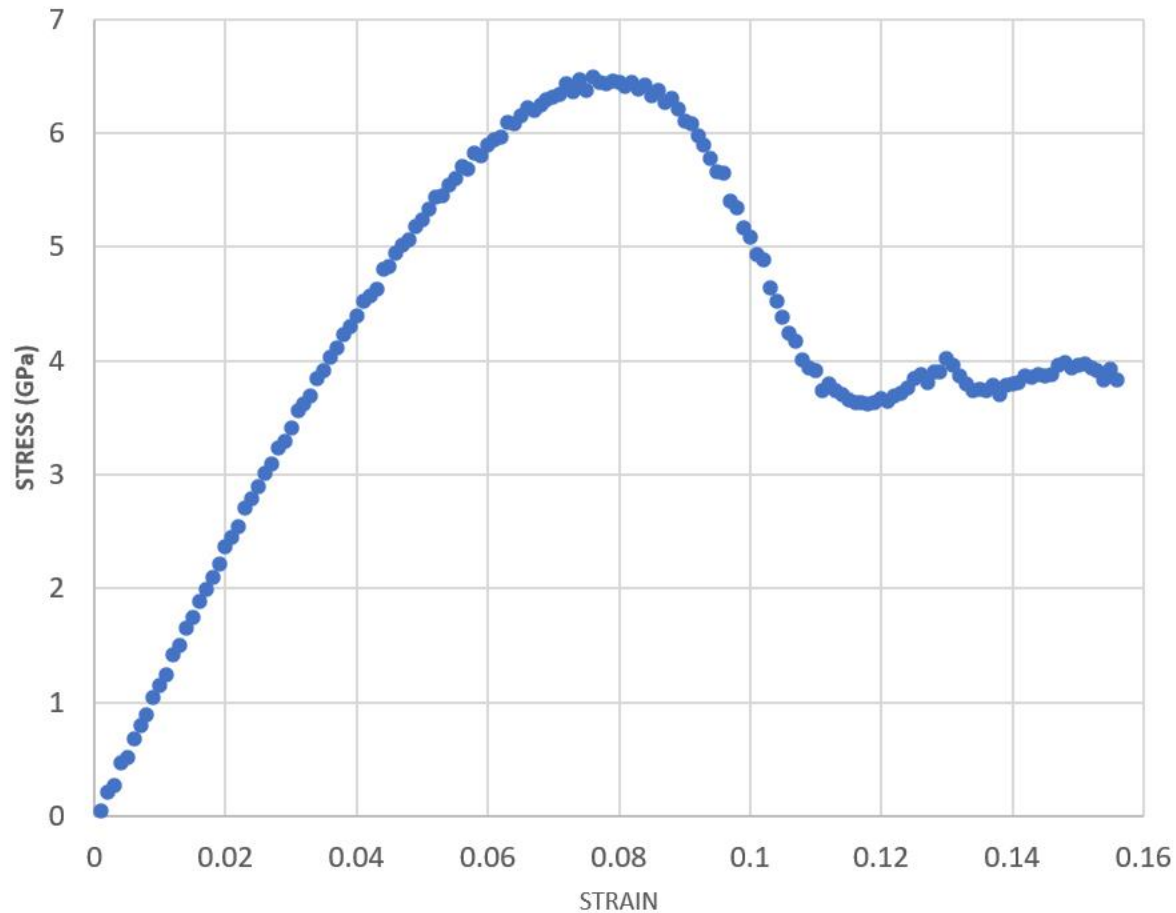

Atomic-Scale Modeling:

➢Application to γ + γ’ Structures

1000K

Ni-Co-Al

HEA-FCC

Al
Co
Cu
Fe
Ni
Cr

Ni-rich Ni-Al

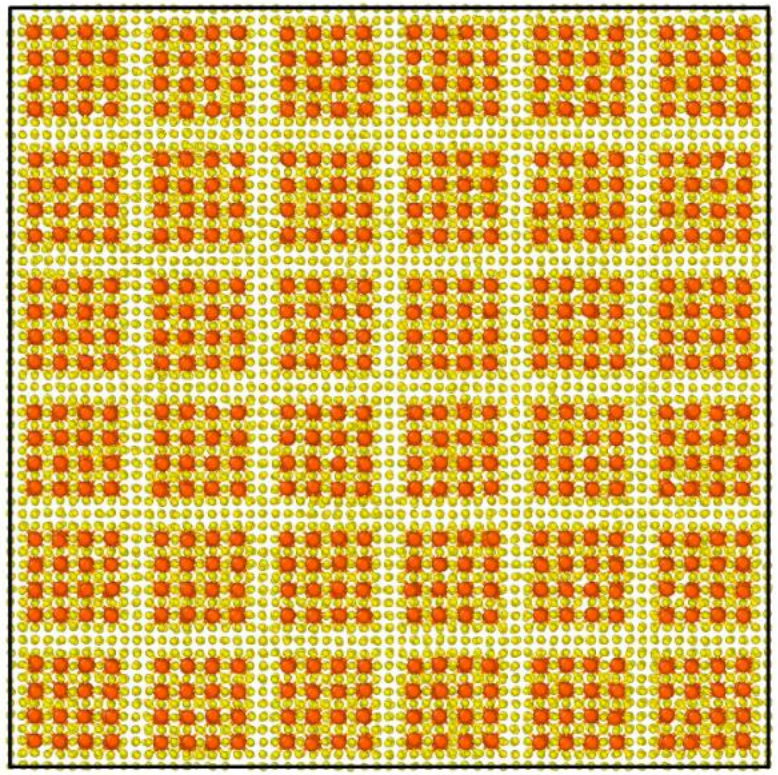

Co-rich Co-Ni-Al

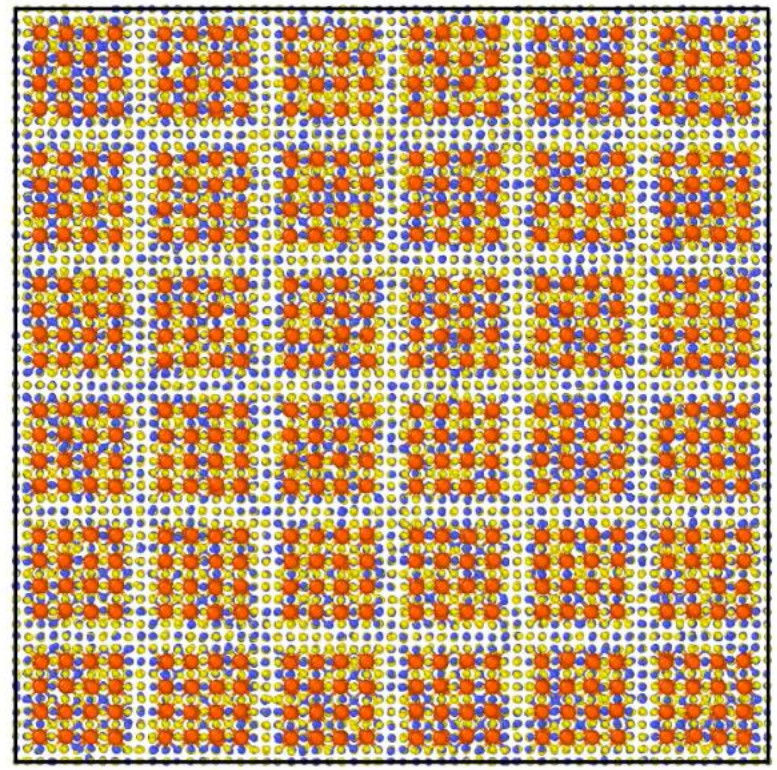

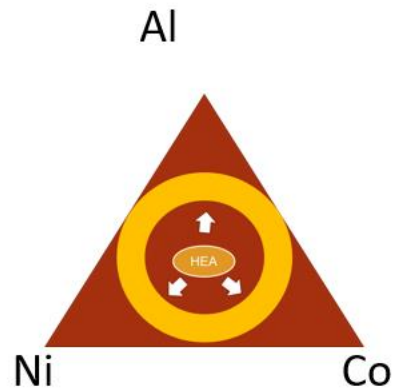

Atomic-Scale Modeling:

- Applications to γ + γ’ structure

Simulated creep tests: **1000K**

$$\sigma_z = 2.0 - 4.0\ GPa$$

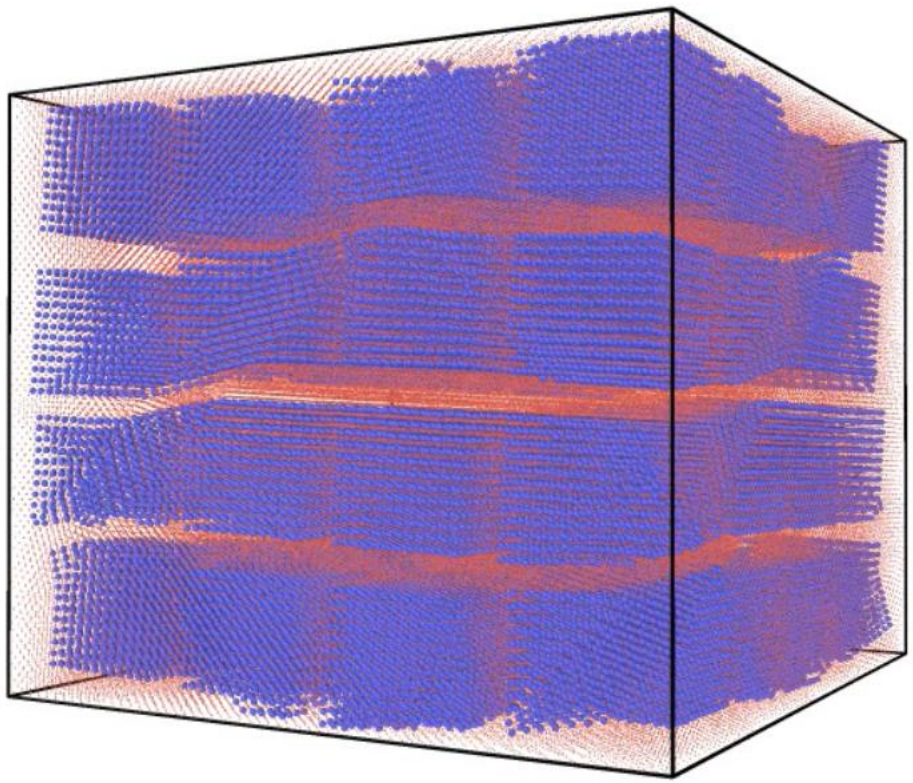

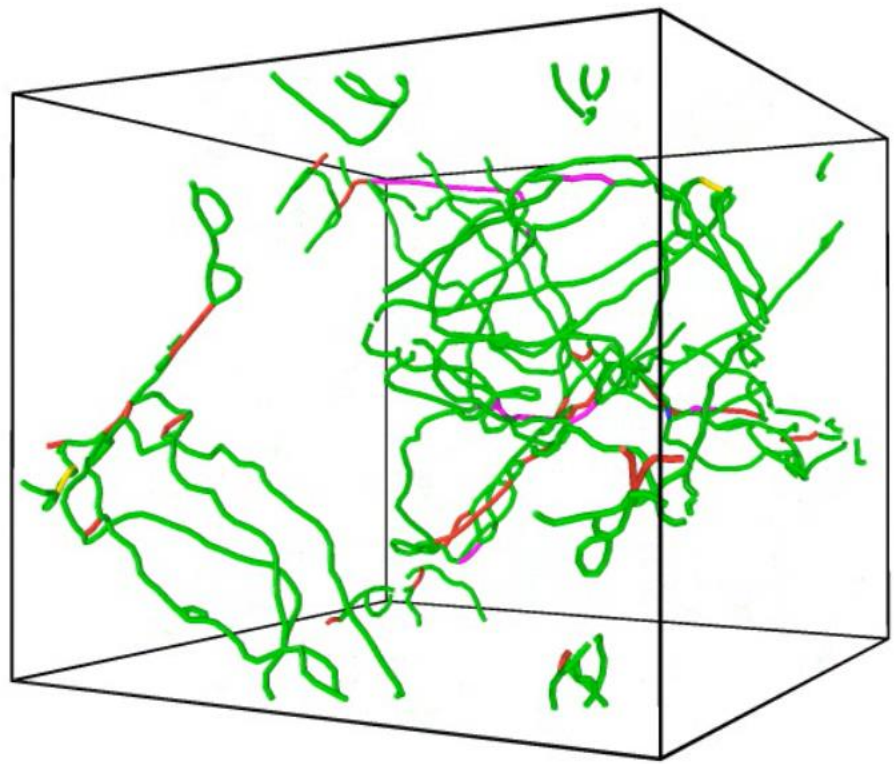

Atomic-Scale Modeling:

- Phase stability analysis

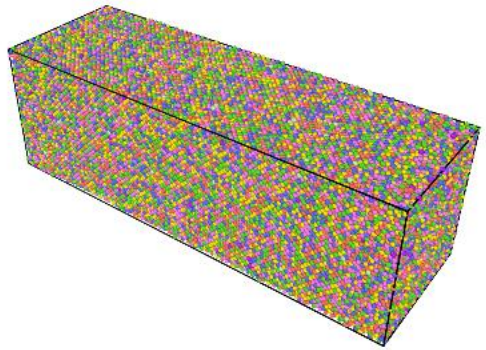

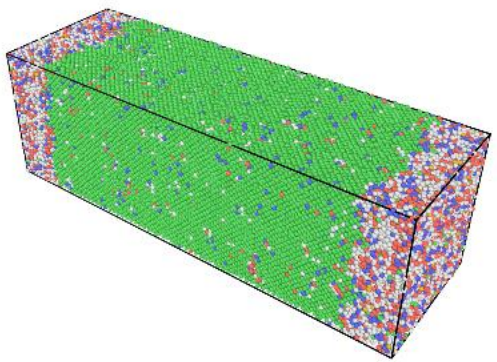

Ni-Al-Cr-Co-Fe-(Ti-Nb) Alloys

Gamma Phase in Ni-based Superalloys/HEA-GGP

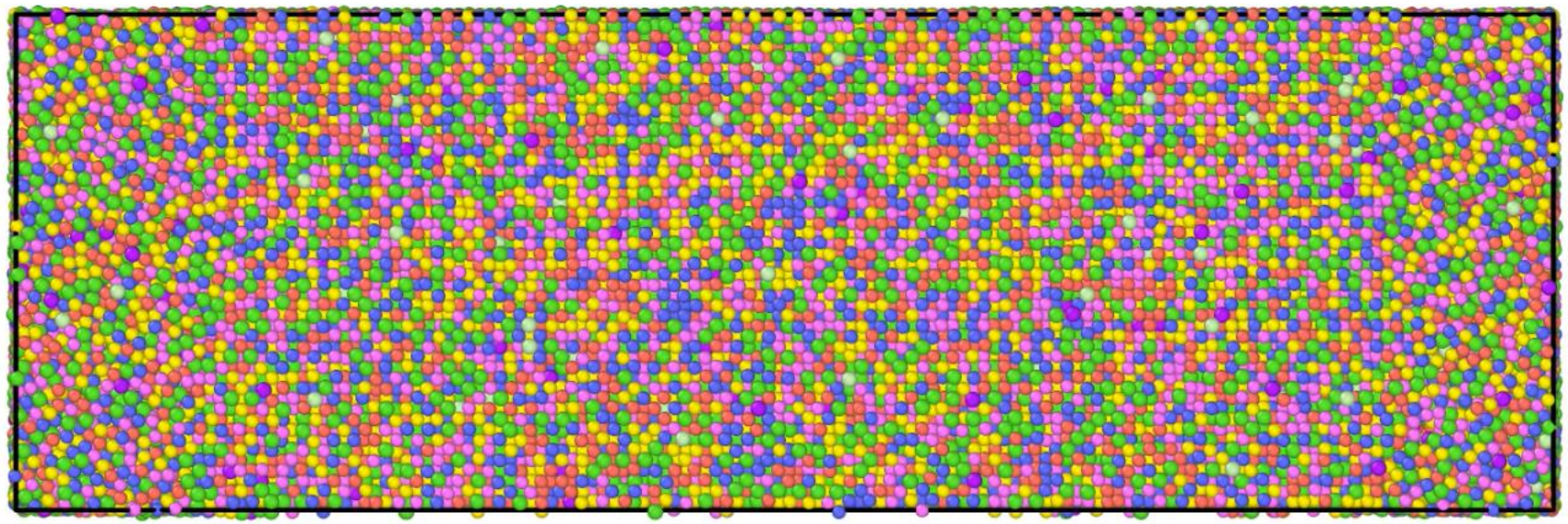

Atomic-Scale Modeling:

- Phase stability analysis

Ni-Al-Cr-Co-Fe-(Ti,Nb) Alloys

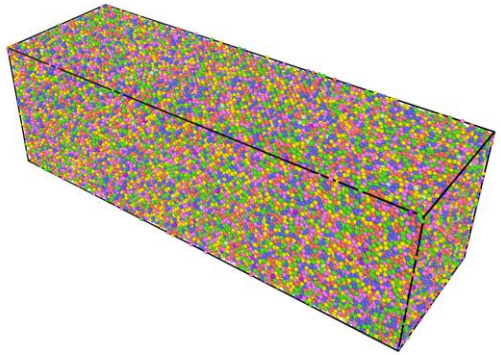

1000K

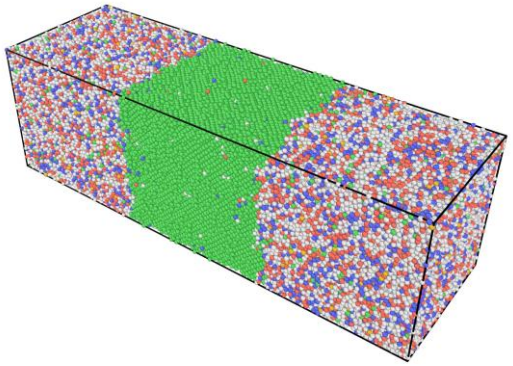

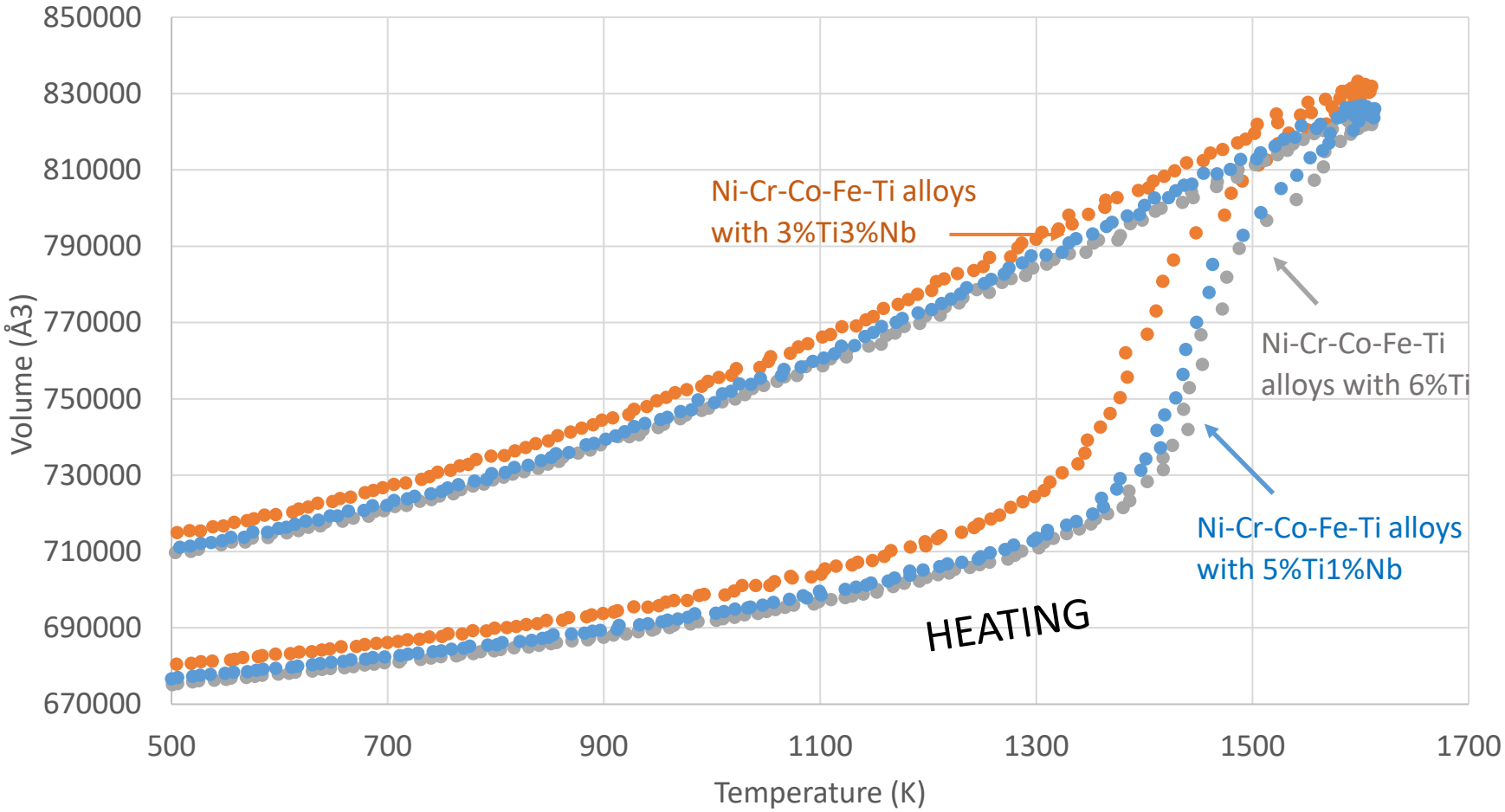

Atomic-Scale Modeling:

➢Phase stability analysis

Ni
Mo
Cr
Fe

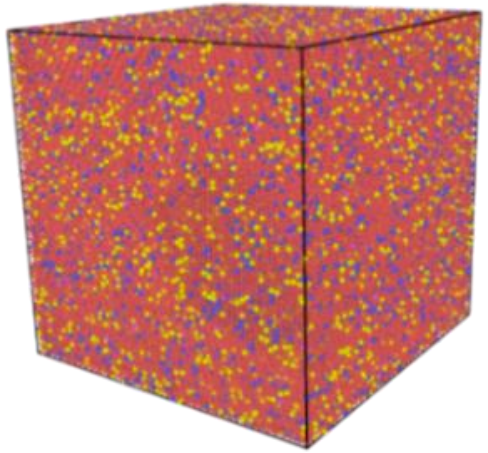

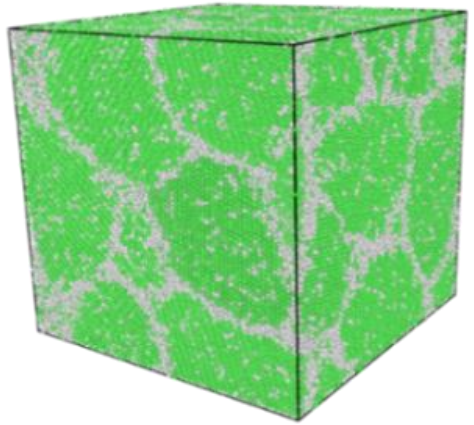

Ni-8.3Cr-10.3Mo-4.43Fe (at. %) quaternary alloy

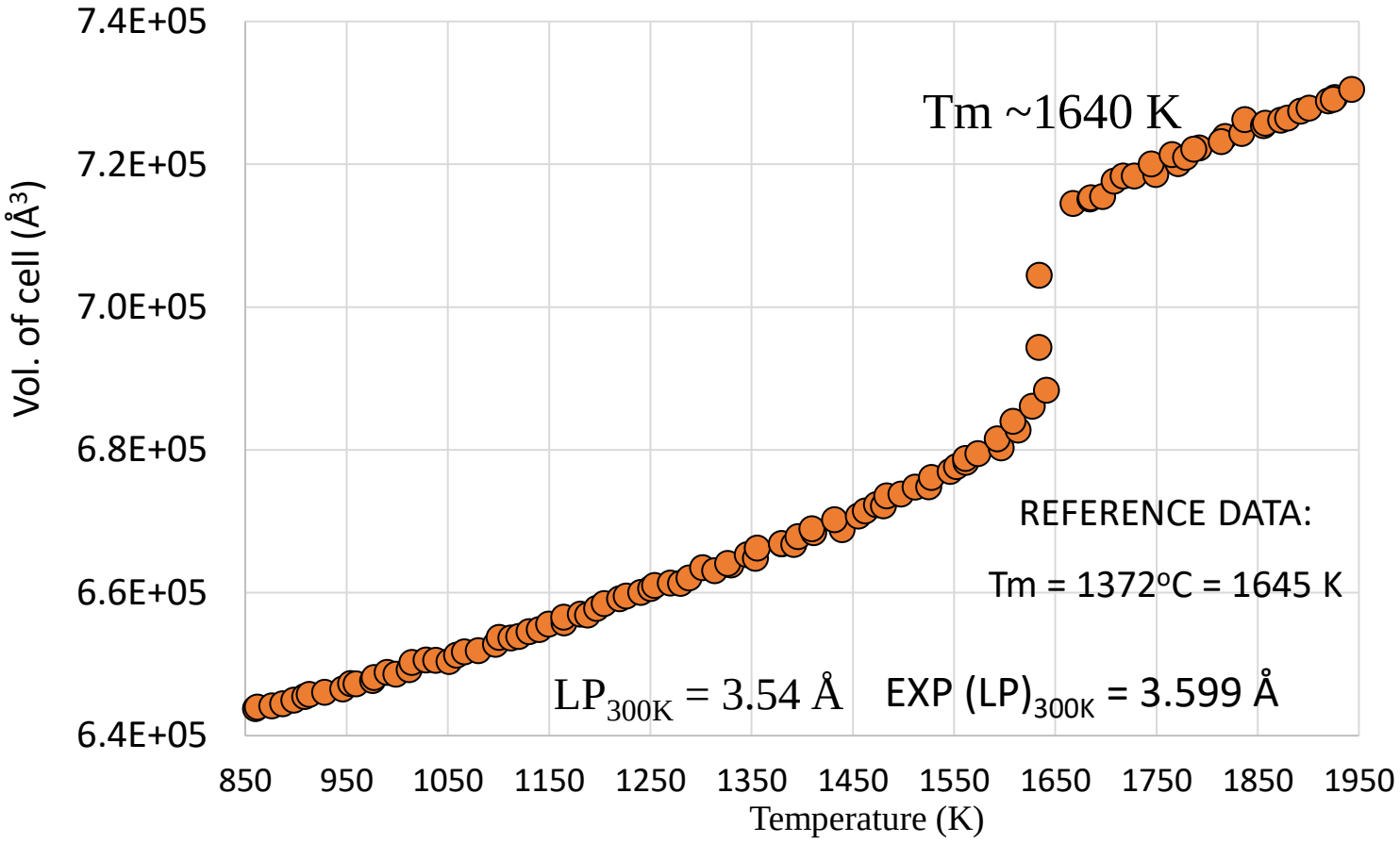

TOP: Snapshot of the atomic trajectories at 1000K

BOTTOM: the same image to mark FCC grain (green) and grain boundaries (white),

Atomic-Scale Modeling:

- Applications to carbide systems

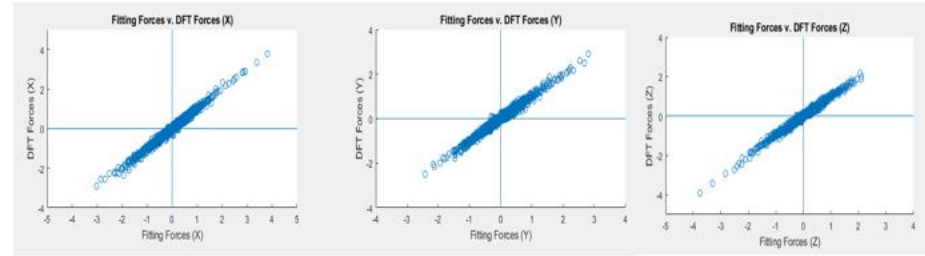

Force matching of DFT vs (M)EAM

Thermal Stability of $M_{23}C_6$

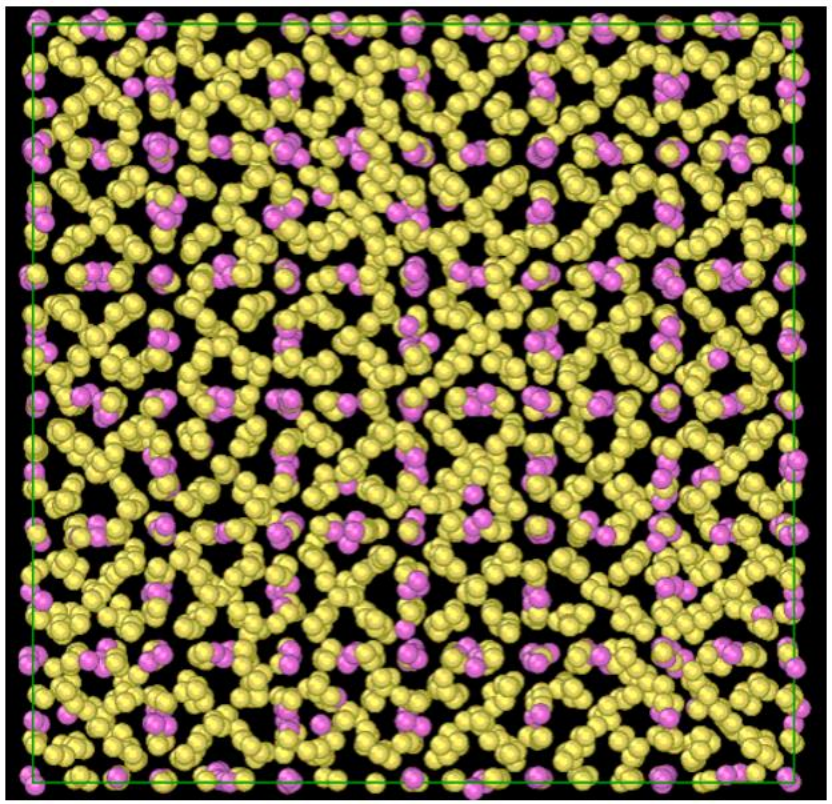

W23C6 @ 2700K

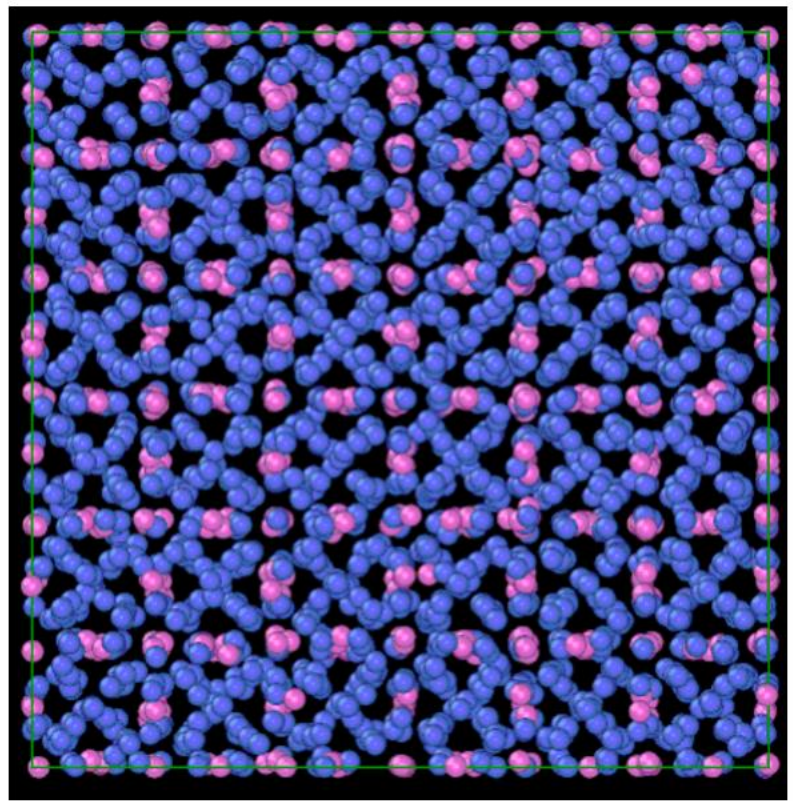

Cr23C6 @ 2100K

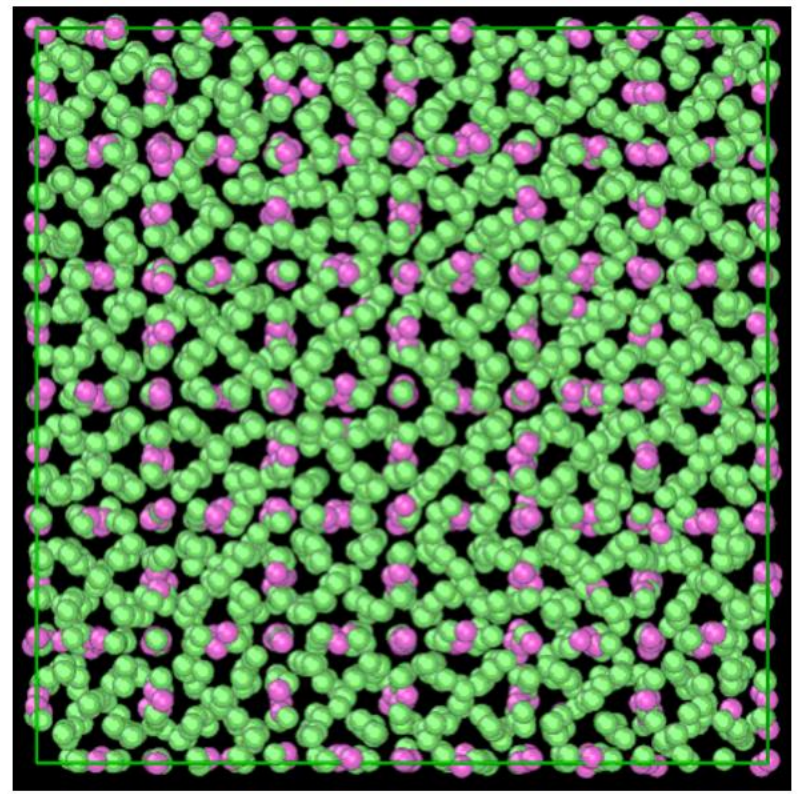

Fe23C6 @ 1800K

Continuum-Scale Modeling:

- Strengthening mechanisms in Ni-Based Superalloys

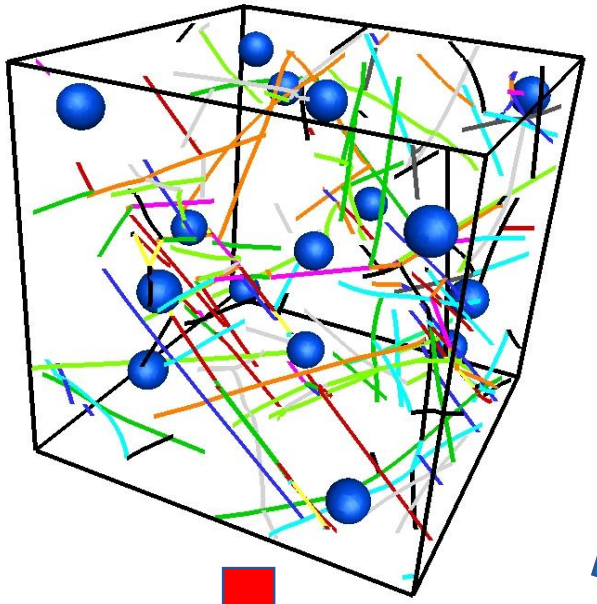

Dislocation interaction

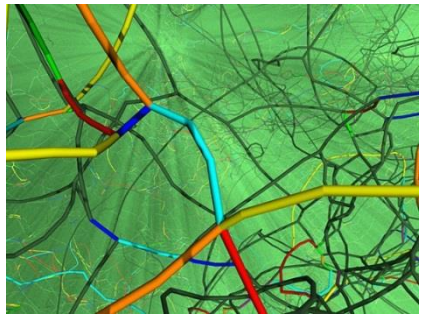

Materials science and technology 25.2 (2009): 213-220.

Dislocation looping

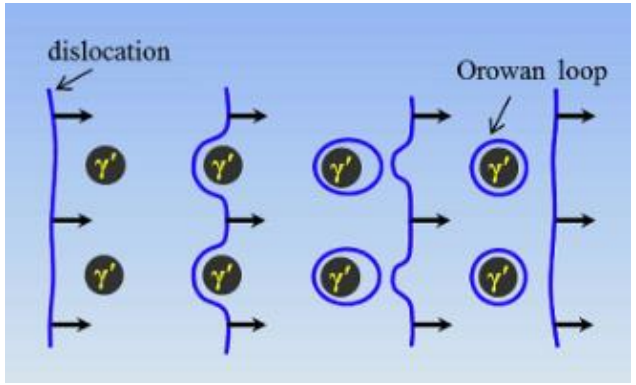

Journal of Alloys and Compounds 687 (2016): 389-401

Dislocation shearing

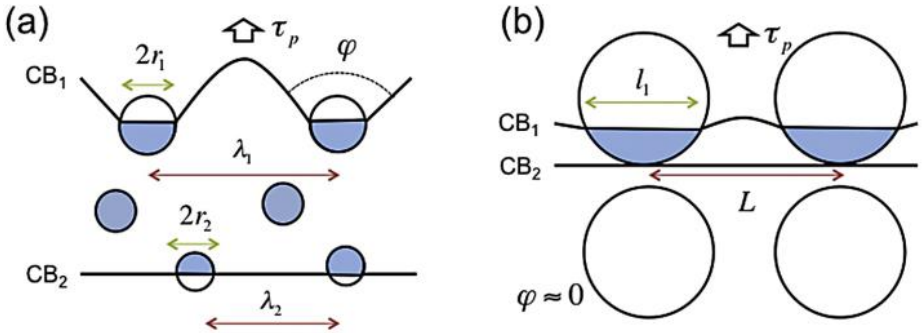

Acta Materialia 98 (2015): 377–390

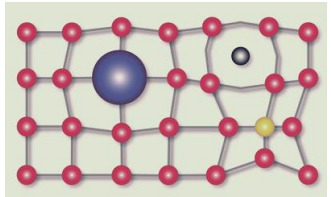

Solid solution

Continuum-Scale Modeling:

➢Strengthening mechanisms in Ni-Based Superalloys

Physical based full-field, dislocation-density based crystal plasticity FE model :

$$\dot{\gamma}^{\alpha}_{slip} = \rho^{\alpha}_{m} * \mathrm{b} * \lambda_{eff} * v_0 * \exp(-\frac{Q_S}{kT}) * \sinh\left[\frac{(\tau^{\alpha} - \tau_{forest+GND} - Min[\tau_{shear}, \tau_{orowan}] - \tau_{ss})b^2\lambda_{eff}}{k_B T}\right]$$

$\rho_m{}^{\alpha}$ is the mobile dislocation density on slip system α, b is burgers vector. k_B is the Boltzmann constant, T is the absolute temperature. $\lambda_{eff}{}^{\alpha}$ is the jump width of slip system α. v_0 is the attach frequency, Q_s is the activation energy for dislocation slip, V is the activation volume.

$$\dot{\gamma}^{\alpha}_{climb} = \rho^{\alpha}_{m} f_p \frac{\lambda_p}{r_p} c_{jog} D_s * \sinh\left[\frac{(\tau^{\alpha} - \tau_{climb})b^2\lambda_p}{k_B T}\right]$$

f_p is the volume fraction of the γ′ phase, λ_p is the average inter-particle spacing and r_p is the average particle radius. c_{jog} is the dislocation line jog density, D_s is the bulk diffusivity.

Continuum-Scale Modeling:

➢Strengthening mechanisms in Ni-Based Superalloys

Physical based full-field, dislocation-density based crystal plasticity FE model :

Mobile dislocation density

$$\Delta\rho_m = \left(\frac{1}{b * \lambda_{eff}} - k1 * \sqrt{\rho_{for}}\right) * \sum_{\alpha} \Delta\gamma^{\alpha}$$

Dislocation Looping

$$\Delta\tau_{orowan} = \frac{0.4\mu b}{\pi * \sqrt{1-v}} * \left(\frac{\ln\left(\frac{2r}{b}\right)}{\lambda_{eff}}\right)$$

Climb dislocations

$$\tau_{climb}{}^{\alpha} = \mu G b \sqrt{\rho_{climb}{}^{\alpha}}$$

Solid solution

$$\tau_{ss} = (1-f)[\sum_{i} (a_i c_i^{\frac{1}{2}})^2]^{1/2}$$

Dislocation Shearing

$$\tau_{shear} = \frac{\gamma_{APB}}{2b} * \frac{l}{\Lambda + d}$$

Dislocation interaction with forest dislocations

$$\tau_{forest} = \chi b \mu \sqrt{\rho_{for} + \rho_{GND}}$$

$$\dot{\gamma}^{\alpha}_{climb} = \rho^{\alpha}_{m} f_p \frac{\lambda_{eff}}{r_{eff}} c_{jog} D_s * \sinh\left[\frac{(\tau^{\alpha} - \tau_{climb} - \tau_{forest+GND}) b^2 \lambda_{eff}}{k_B T}\right] * sign(\tau^{\alpha})$$

$$\begin{cases} 0, & |\tau^{\alpha}| \le \tau_{climb} + \tau_{forest+GND} \\ \dot{\gamma}^{\alpha}_{climb}, & \tau_{climb} + \tau_{forest+GND} \le |\tau^{\alpha}| \le Min[\tau_{shear}, \tau_{orowan}] + \tau_{forest+GND} \\ \dot{\gamma}^{\alpha}_{slip}, & |\tau^{\alpha}| \ge Min[\tau_{shear}, \tau_{orowan}] + \tau_{forest+GND} \end{cases}$$

$$\dot{\gamma}^{\alpha}_{slip} = \rho^{\alpha}_{m} * b * \lambda_{eff} * v_0 * \exp(-\frac{Q_S}{kT}) * \sinh\left[\frac{(\tau^{\alpha} - \tau_{forest+GND} - Min[\tau_{shear}, \tau_{orowan}]) b^2 \lambda_p}{k_B T}\right] * sign(\tau^{\alpha})$$

Continuum-Scale Modeling:

➢Strengthening mechanisms in Ni-Based Superalloys

- The constitutive formulations are written as a user-defined material (UMAT) subroutine in Abaqus software.
- The dislocation density evolution calibrated with the stress-strain curve with experimental results for of Haynes 282 from reference (Zhao, Shen, Niezgoda, & Wang, 2018):

Symbol	Value	Meaning
Q_{slip}	3.7×10^{-19} J	Activation energy for slip
f_p	0.11	Volume fraction
v_0	7.8×10^{11}	Attack frequency
η	0.65	Spatial-distribution parameter
k_1	3.0×10^{9} m^{-1}	Coefficient for statistical trapping of mobile dislocations
k_3	50.0	Coefficient for climb dislocation density deposited
χ	0.15	Dislocation interaction factor
b	2.54×10^{-10}nm	Magnitude of Burger's vector
γ_{APB}	0.18 J	Anti-phase boundary energy
β_{for}	0.01	Constant relate to the spacing of forest dislocation
β_{GND}	1.0	Constant relate to the spacing of GND
β_p	0.55	Constant relate to the spacing of precipitates

Validation of the slip model:

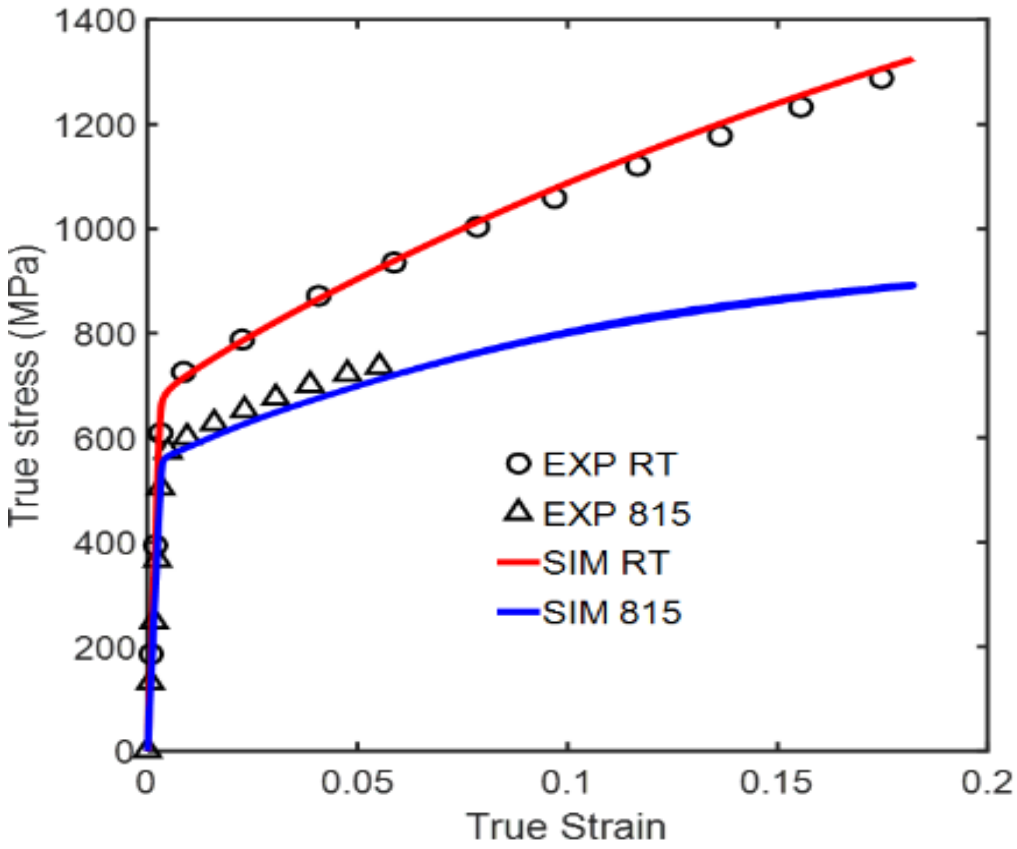

Comparison of the predicted stress-strain curves under different temperatures with experimental data from International Journal of Plasticity 109 (2018) 153–168.

Summary

Modeling at electronic structures:

- Completed fundamental DFT-based materials property database for $M_{23}C_6$
- To finish fundamental DFT-based materials property database for mixed phases/interfaces (γ+ γ') in Q3-Q4

Modeling at atomic scale:

- Developed working interatomic potentials designed for γ + γ' and carbide phases
- To complete verifications on multi-component interatomic potentials for γ + γ' matrix in Q3
- To complete verifications on multi-component interatomic potentials for carbide precipitates in Q3
- To complete verifications on multi-component interatomic potentials for γ + γ' matrix//carbides in Q4

Modeling at continuum scale:

- Developed framework for semi-empirical crystal plasticity models on void deformation at grain boundaries
- Developed framework for semi-empirical crystal plasticity models for γ + γ' matrix
- To complete validations on the semi-empirical dislocation density -based crystal plasticity models in Q3-Q4

Path forward

Artificial Intelligence (AI) Applications to Multi-modal Modeling Approaches:

INTERCONNECTED MATERIALS DATABASE THROUGH
AI-DRIVEN APPLICATION PROGRAMMING INTERFACE (API)s

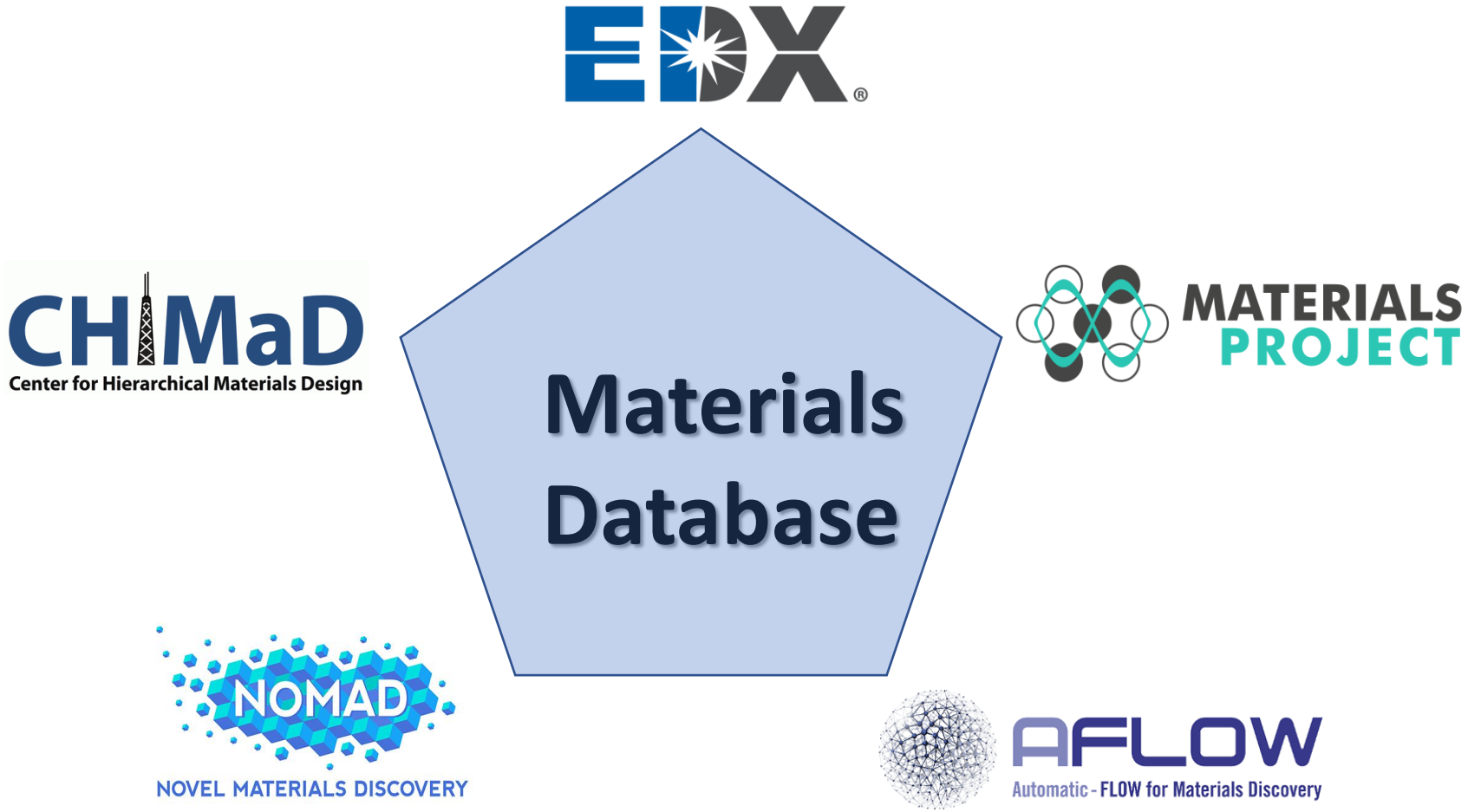

Path forward

Artificial Intelligence (AI) Applications to Multi-modal Modeling Approaches:

DEEP LEARNING POTENTIAL AT ATOMISTIC SCALE

Examples: Carbide phase ($Fe_{23}C_6$)and boride phase (ZrB_2)

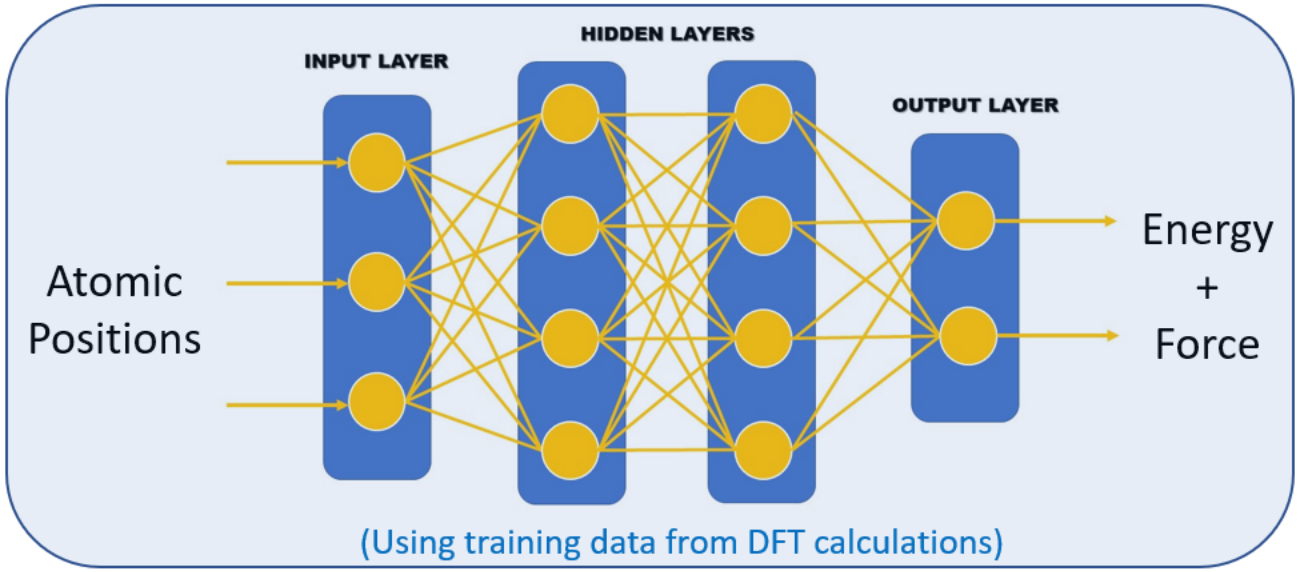

High-Temp. Stability Tests:

$Fe_{23}C_6$

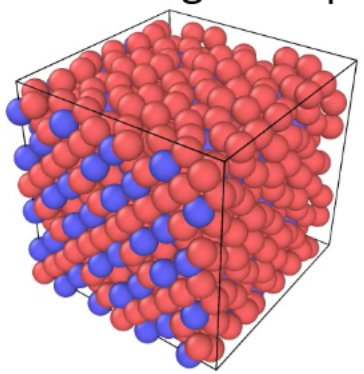

600K

ZrB_2

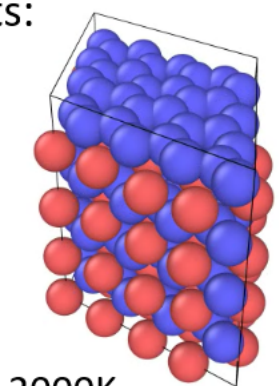

1500-2000K

Phonon Dispersion Curves

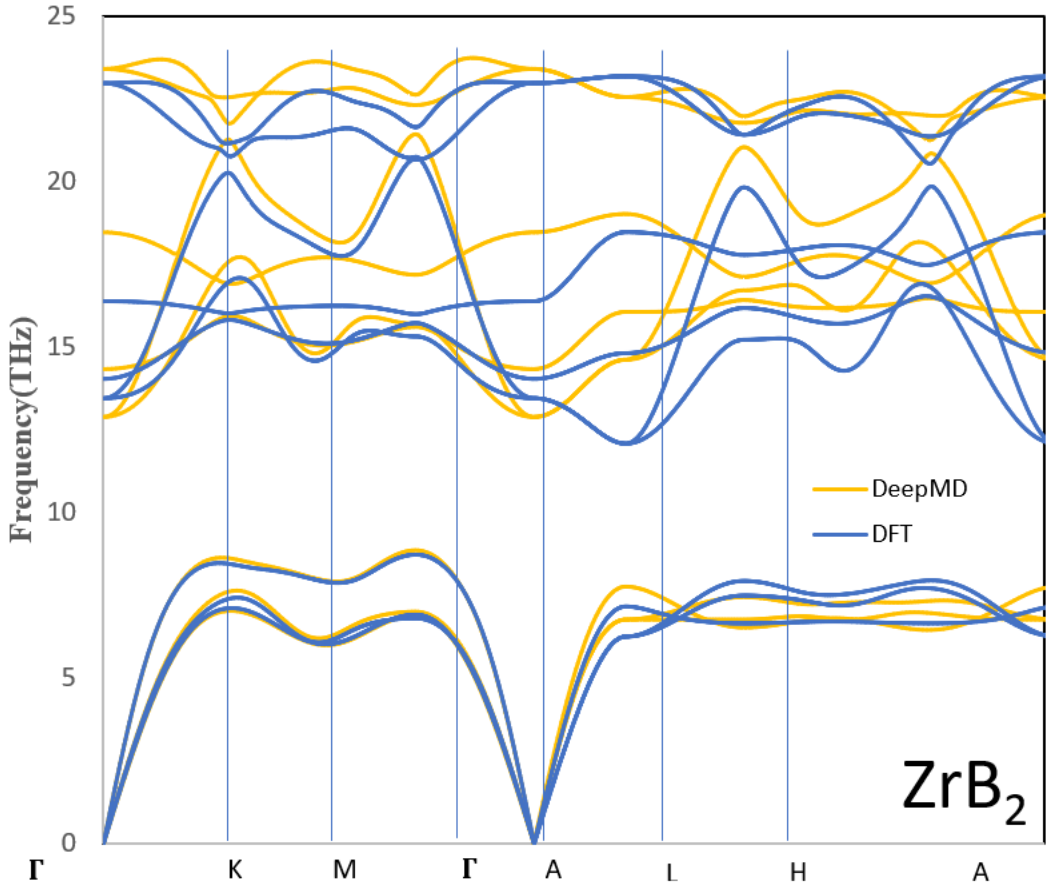

Path forward

Artificial Intelligence (AI) Applications to Multi-modal Modeling Approaches:

DEFORMATION DYNAMICS AT ATOMISTIC SCALE

DISLOCATION POPULATION –BASED ANALYSIS

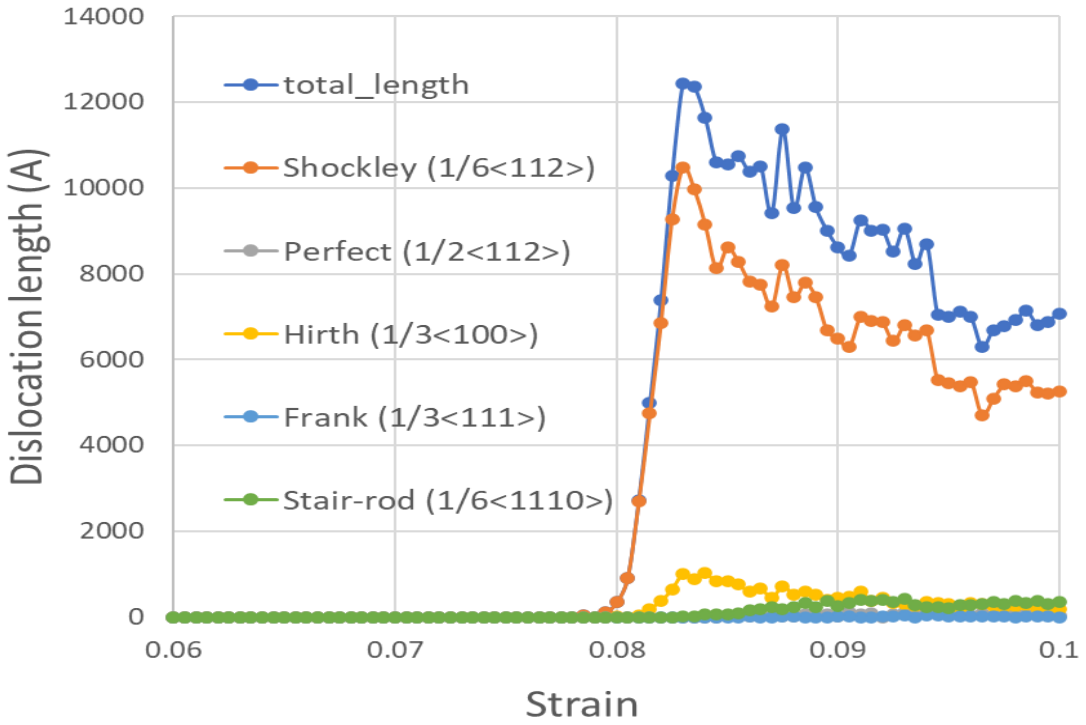

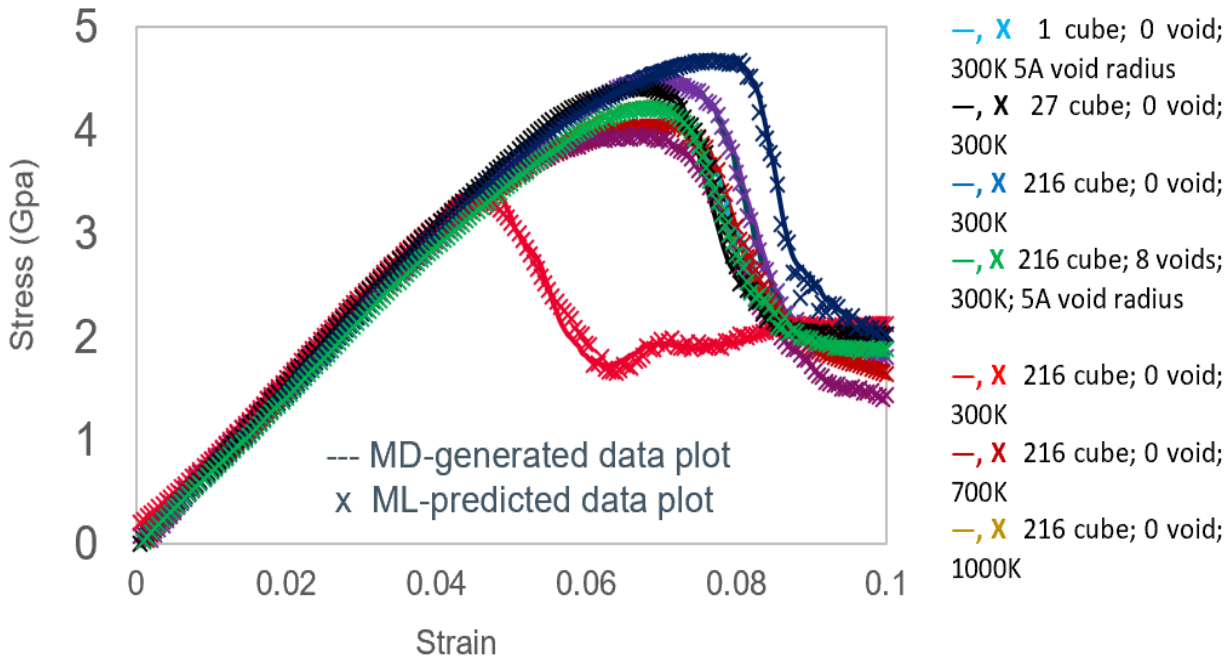

Thank You